Proc. Natl. Acad. Sci. USA
Vol. 82, pp. 8463–8467, December 1985
Biophysics

Analysis of optical spectra from single crystals of *Rhodopseudomonas viridis* reaction centers

(dichroism spectra/crystallized reaction center/excitons/protein–pigment interaction/photosynthesis)

E. W. KNAPP*, S. F. FISCHER*, W. ZINTH*, M. SANDER*, W. KAISER*, J. DEISENHOFER†, AND H. MICHEL†

*Physik-Department der Technischen Universität München, D-8046 Garching and D-8000 München, Federal Republic of Germany; and †Max-Planck-Institut für Biochemie, D-8033 Martinsried, Federal Republic of Germany

Communicated by Rudolph A. Marcus, August 9, 1985

ABSTRACT **Absorption spectra and light-induced absorbance changes of crystals from *Rhodopseudomonas viridis* reaction centers are recorded. A theoretical analysis of the absorption and circular dichroism spectra is presented, yielding a consistent picture of spectroscopic and structural information.**

The primary process in bacterial photosynthesis involves a light-driven electron transfer across a membrane. It is catalyzed by a protein–pigment complex, the photosynthetic reaction center (RC). The chemical nature and pigment composition are known for a number of RCs (1–4). The RC from the purple photosynthetic bacterium *Rhodopseudomonas viridis* was crystallized (5); the RCs in those crystals are photochemically active (6). Recently, an x-ray structure analysis at 3 Å resolution provided the detailed arrangement of the pigments in the RC (7) [four bacteriochlorophyll b (BC), two bacteriopheophytin b (BP), and four heme groups]. The heme groups are bound to a *c*-type cytochrome. The BCs and BPs are associated with the protein subunits L and M, respectively, and are indexed in this paper by L and M accordingly. These pigments are arranged in two branches, which exhibit an approximate 2-fold rotation symmetry (7). At the axis of rotation, two BCs interact closely (Mg–Mg distance, ≈7 Å) with their pyrrole rings I stacked on top of each other. They form the special pair and are denoted BC_{LP} and BC_{MP}. Next to the special pair are the so-called accessory monomers BC_{LA} and BC_{MA}. The Mg–Mg distance between the BC in the same branch is ≈11 Å. In close proximity to the BC_As are the two BPs at the end of the branches. The distance of the ring centers of BP and BC_A from the same branch is ≈11 Å. The approximate 2-fold rotation symmetry is broken by the presence of only one quinone, probably menaquinone, at the end of the L branch; apparently, the RC's second quinone was lost during purification or crystallization.

In this paper, we investigate absorption spectra and absorbance changes after illumination with actinic light by using single crystals of different orientations. This yields a considerable increase of information as compared to spectra from RC in solution. Circular dichroism (CD) spectra of reaction centers in solution are also considered (8, 9). The spectra are analyzed by using the structural information of the RCs (7). (See also figure 1 in ref. 10.)

Materials and Methods

The isolation of the reaction centers and the crystallization procedure has been described (5, 6). During the investigation, the crystals were kept in closed cells containing buffer solution (6). Thin crystal platelets (≈0.2 mm × 0.1 mm × 20 μm) with the smallest extension in the x or y direction and (0.1 mm × 0.1 mm × 20 μm) with the smallest extension in the z direction were occasionally obtained by crystallization methods. They were used in the transmission experiments, allowing absorption measurements along different crystallographic directions. The crystals belong to the tetragonal space group $P4_32_12$. For tetragonal crystals, it is sufficient to consider two geometries for the absorption measurements where the electric field vector E of the light is parallel ($E_{\parallel}$) or perpendicular ($E_{\perp}$) to the tetragonal z axis, respectively. Absorption spectra of other geometries can be derived from the results of these two spectra.

The transmission measurements are performed by using two spectrometers (resolution, 3 nm), polarizing optics, a microscope, photomultipliers, and phase-sensitive detection. Care was taken to keep the measuring at the lowest possible level to minimize absorption changes due to the photochemical activity of the reaction centers. For that reason, the first spectrometer of a small spectral bandwidth (3 nm) was used before the sample. The second spectrometer just in front of the photomultiplier was used to reject stray light and the light of the actinic radiation. The actinic light source was a Xenon arc lamp in conjunction with a spectrometer (960 nm < λ < 980 nm). The intensity level of the exciting light was kept sufficiently low to ensure a linear dependence of the absorbance change on the light intensity.

Experimental Results

Transmission spectra of a thin crystal of the reaction centers are shown in Fig. 1 for two different geometries. They display a strong dichroism. The Q_y bands of the pigments are between 750 and 1000 nm and the Q_x bands are between 500 and 650 nm. The broad band at 960 nm is due to the special pair BCs. The band around 830 nm belongs to the accessory BC and the BP. The Q_x bands of the BC pigments are at 610 nm. Around 550 nm, the Q_x bands of the BP molecules and the α bands of the *c*-type cytochromes appear.

The absorption band of the special pair (960 nm) can be bleached by illumination with strong actinic light, causing charge separation in the RC. A positive charge is left at the special pair and a negative charge is transferred to the quinone. This process is accompanied by absorbance changes in the whole spectral region. The light-induced absorbance changes are presented in Figs. 2 and 3 for two geometries (11).

Theoretical Methods

The spectral properties of the porphyrins in the central part of the reaction center containing four BCs and two BPs are calculated independently for the Q_y and Q_x bands. We use an

The publication costs of this article were defrayed in part by page charge payment. This article must therefore be hereby marked "*advertisement*" in accordance with 18 U.S.C. §1734 solely to indicate this fact.

Abbreviations: RC, reaction center; CD, circular dichroism; BC, bacteriochlorophyll b; BP, bacteriopheophytin b.

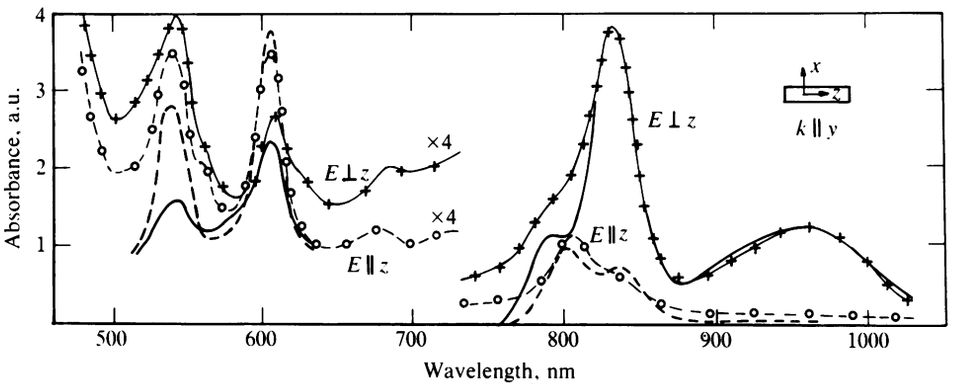

FIG. 1. The absorption spectrum of the Q_y and Q_x bands is shown from crystals of the reaction center at 300 K. The geometry of the observation is indicated in the *Inset*. Experimental data are shown by symbols connected with lines; theoretical data are shown by solid lines. In the Q_x bands, a constant base line of 0.2 arbitrary unit (a.u.) has been added to the calculated values.

elementary theory (11, 12) where the local excitation at pigment n is characterized by a single state $|n\rangle$ of energy E_n. Any two states $|n\rangle$, $|m\rangle$ are coupled via interaction matrix elements $V(n,m)$. The hamiltonian describing the exciton states of such a system of N coupled chromophores can be written as follows

$$H = \sum_{n=1}^{N} |n\rangle E_n \langle n| + \sum_{m\neq n=1}^{N} |n\rangle V(n,m) \langle m|. \quad [1]$$

The interaction energies $V(n,m)$ (Table 1) are calculated with an extended dipole model where charges of opposite sign are situated at the appropriate N atoms in the inner part of the porphyrins. A calculation based on point dipoles gives very similar results. The interaction between pigments from different RCs are neglected. Their minimum distance in the crystal is >50 Å (7). The absorption spectra can be expressed in terms of the N eigenvalues $\hbar\omega^{(k)}$ (k = 1,2...N) and the corresponding transition dipole moment vectors $\nu^{(k)}$. The latter relate to the transition dipole moment vectors $\mu^{(n)}$ of the individual pigments (n) via a transform using the eigenvectors $e^{(k)} = (e_1^{(k)}, \ldots, e_N^{(k)})$ of the hamiltonian Eq. 1

$$\nu^{(k)} = \sum_{n=1}^{N} e_n^{(k)} \mu^{(n)}. \quad [2]$$

The extinction coefficients are written as

$$\varepsilon_{\parallel z}(\omega) \approx \omega \sum_{k=1}^{N} (\nu_z^{(k)})^2 \delta(\omega - \omega^{(k)}) \quad [3]$$

and

$$\varepsilon_{\perp z}(\omega) \approx \omega \sum_{k=1}^{N} 1/2[(\nu_x^{(k)})^2 + (\nu_y^{(k)})^2] \delta(\omega - \omega^{(k)}), \quad [4]$$

for light polarized parallel and perpendicular to the z direction, respectively. The absorbance changes are calculated as difference of absorption spectra before and after illumination with actinic light. To relate the experimental data with the calculation, the crystal symmetry must be considered explicitly.

Similarly, the ellipticity of the CD spectrum (13) reads

$$\theta(\omega) \approx \omega^2 \sum_{k=1}^{N} \delta(\omega - \omega^{(k)}) \sum_{i,j=1}^{N} (\mathbf{Q})_{ij} e_i^{(k)} e_j^{(k)}. \quad [5]$$

The matrix elements $\mathbf{Q}_{ij}$ in Eq. 5 are given in terms of the transition moment vectors $\mu^{(i)}$ and the distance vector R_{ij} of the pigments i and j,

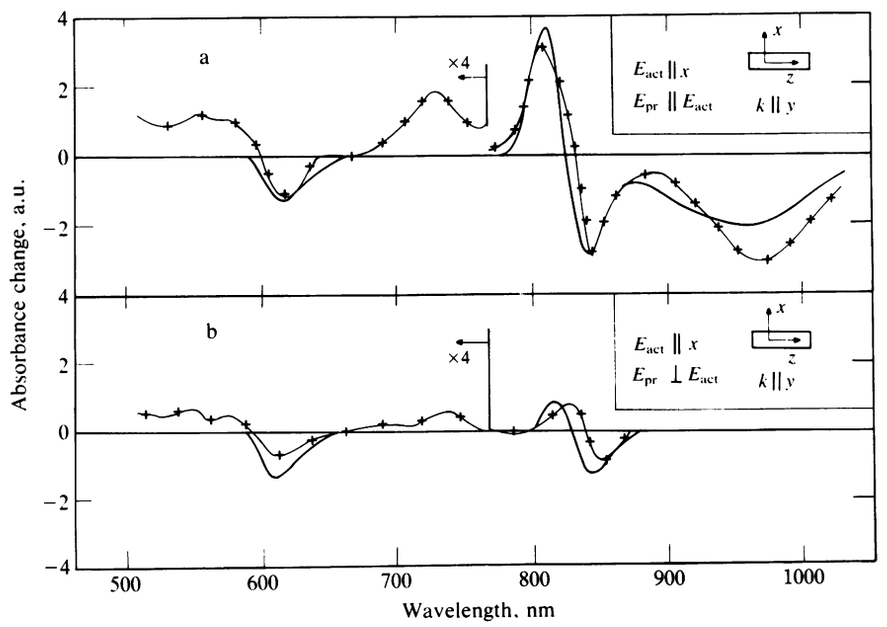

FIG. 2. Absorbance change of the crystallized RC upon illumination with actinic light at 970 nm. The geometry is indicated in the *Inset*. The polarization of probing and actinic light is parallel (*a*) and perpendicular (*b*) to each other. +—+, Experimental data; —, theoretical data. E_{act} and E_{pr} are the electric field vectors of actinic and probing light, respectively. Both have the wave vector k in the same direction. All theoretical and experimental absorbance changes displayed have a fixed normalization with respect to each other.

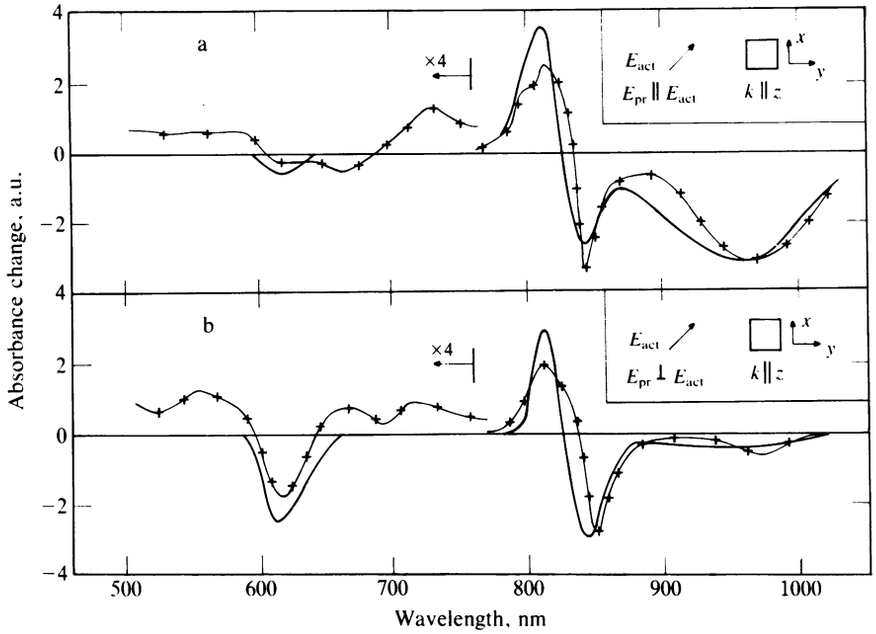

FIG. 3. Absorbance change of the crystallized RCs. The geometry is indicated in the *Inset*. Other details are the same as in Fig. 2.

$$(\mathbf{Q})_{ij} = \mu^{(i)} \cdot R_{ij} \times \mu^{(j)}. \quad [6]$$

Note that in this frame the CD spectrum is conservative—i.e., the ellipticity averaged over the whole frequency regime vanishes

$$\int \theta(\omega) \frac{d\omega}{\omega^2} = \sum_{i,j=1}^{N} (\mathbf{Q})_{ij} \sum_k e_i^{(k)} e_j^{(k)} = \sum_{i,j} (\mathbf{Q})_{ij} \delta_{ij} = 0. \quad [7]$$

To facilitate a comparison with the experimental data, the individual sharp δ function lines of the theoretical spectra (Eqs. 3–7), are replaced by suitable gaussian profiles whose widths are given in Table 2.

Model Parameters

The parameters of the model are the excitonic interactior energies $V(n,m)$ between different pigments and the diagonal energy shifts E_n. The excitonic interaction energies are calculated with an extended transition dipole model, where charges of opposite sign are placed at the nitrogen atoms of the pyrrole rings I and III (II and IV) for the Q_y (Q_x) bands of the BC and BP molecules. Corrections to the transition dipole model can become important for pigment distances <3 Å (14). With the exception of the special pair monomers, the distances are much larger than 3 Å. In ref. 9, the transition dipole moment of the Q_y bands of BC b and BP b monomers was given as $30D^2$ and $19D^2$, respectively. We have used these values in a recent paper (10). In this work, the transition moments have been raised to $45D^2$ and $30D^2$, respectively, to reproduce the absolute value of the CD spectrum of RCs within 15%. The larger values are also consistent with the fact that the transition moment of the Q_y bands is larger for BC b monomers than it is for BC a monomers, where its value is $41D^2$ (15). The dipole interactions belonging to the Q_x bands are ≈10% of the interactions in Q_y bands (4) and are assumed to be equal for BC b and BP b monomers.

Table 1. Exciton interaction energies (cm^{-1}) $V(n,m)$, for the Q_x bands (upper right) and the Q_y bands (lower left)

	Q_x					
Q_y	BP_M	BC_{MA}	BC_{MP}	BC_{LP}	BC_{LA}	BP_L
BP_M	2200 500	9	−8	−2	−1	1
BC_{MA}	150	0 0	−8	6	−1	0
BC_{MP}	−9	−35	−200 −845	69	7	−2
BC_{LP}	33	−173	905	−200 −845	−12	−7
BC_{LA}	−11	30	−195	−22	0 0	11
BP_L	6	−11	37	−10	193	1800 200

A dipole strength of 45 D^2 for BC (30 D^2 for BP) and 4.5 D^2 for BC and BP has been assumed for the Q_y and Q_x bands, respectively. A constant term of 12,140 cm^{-1} and 16,500 cm^{-1} must be added to all diagonal energies of the Q_y and Q_x bands, respectively. The nomenclature is explained in the Introduction.

The broad absorption peak at 965 nm is the low energy band of the special pair BC_Ps. It is ≈1750 cm^{-1} below the absorption peak of the accessory BC_As at 830 nm. Only part of this energy shift is due to the band splitting of the special pair from the transition dipole interaction V_p = 905 cm^{-1}. This shift can be accounted for by diminishing the diagonal energies of the special pair BC_Ps to a value E_p = −845 cm^{-1} below the diagonal energies of the BC_As. The mechanism for this specific energy shift may be protein–pigment interactions (16), charge transfer interactions, or pigment–pigment interactions as, for instance, Davydov's D term (17).

In solution, the excitation of the Q_y (Q_x) bands of the BP monomers are ≈400 cm^{-1} (2000 cm^{-1}) higher than for the BC monomers (3, 19). This has motivated the upward shift of the corresponding diagonal elements of the interaction matrix (Table 1). The actual energy values are adjusted to the polarized absorption spectrum (Fig. 2). They differ probably because of interactions with the protein. The spectra of absorbance change also require determination of the excitonic states of the RC after illumination. After illumination, a positive charge is delocalized over the two BC_P. The presence of the charge changes the diagonal energies of the excitation at the BC_P monomers drastically, so that they now absorb in

Table 2. Energies, intensities, polarization, and composition of the exciton states in the Q_y band

Energy eigenvalue, nm	Intensity, units of BC b monomer	Major polarization axis	Monomer contributions to the exciton states, %					
			BP_M	BC_{MA}	BC_{MP}	BC_{LP}	BC_{LA}	BP_L
964*	2.08	$\perp z$	0	0	50	50	0	0
838†	1.00	$\perp z$ ($\parallel z$)	1	14	16	19	41	9
830†	1.24	$\perp z$	4	56	4	1	24	11
811‡	0.20	$\perp z$ ($\parallel z$)	3	20	24	25	1	27
801†	0.30	$\parallel z$	0	2	6	5	34	53
788†	0.50	$\perp z$	92	8	0	0	0	0

Gaussian line shapes have been assumed. At the low-energy side, the width is 500 cm^{-1}*, 240 cm^{-1}†, or 780 cm^{-1}‡. At the high-energy side, the width is 780 cm^{-1}*, 240 cm^{-1}†, or 500 cm^{-1}‡.

another frequency regime. Consequently, the exciton states of the charged special pair do not interact with the states of the other pigments and are therefore omitted. The presence of the positive charge at the special pair can increase the diagonal energy of the nearby BC_A monomers. When the BP monomers carry a negative charge, the observed energy shift is $\approx$200 cm^{-1} (20). A similar shift is expected in the present case. The diagonal energy of the BC_A is raised accordingly (Table 1).

The Absorption Spectra

The absorption spectrum of RCs of *R. viridis* is shown in Fig. 2. The rather broad exciton state at 960 nm is the low-energy special pair state P(−) polarized perpendicular to the z direction. It carries the intensity from both BC_P monomers (Table 2). The next two higher exciton states (bands around 830 nm) correspond to the two accessory monomers BC_A. Both are polarized mainly perpendicular to the z direction and borrow additional intensity from the BP monomers. The highest exciton states that carry significant intensity are due to the two BP monomers. Some intensity from the BPs appears in the exciton states at lower energies. The BP_M is polarized perpendicular and BP_L is polarized parallel to the z direction.

The absorption spectrum with polarization perpendicular to the z axis exhibits a shoulder at 790 nm, whereas the spectrum with polarization parallel to the z axis has a maximum at 805 nm. Since we know experimentally and theoretically the polarization of the BP molecules, we can conclude that BP_M is responsible for the shoulder at 790 nm in the spectrum with $E \perp z$. Its diagonal energy is larger than the energy of the BP molecule in the other branch, as given in Table 1. The shoulder at 840 nm in the spectrum with $E \parallel z$ is due to the exciton state BC_{LA}, which also carries some intensity polarized along the z axis.

The Exciton States of the Special Pair

The upper exciton state P(+) of the special pair has been the subject of extensive discussions (3, 9, 18, 20, 21). This state can be involved in the charge separation, the first step of the electron transfer process, which is important for the function of the RC. In particular, a special pair state with an energy near the accessory monomers can support the charge separation. The detailed polarization experiments and the model calculations based on the structural information allow us to solve this problem. The transition dipole moment vectors of the Q_y bands of the special pair BC_Ps are approximately antiparallel with an angle of 151° and provide a positive interaction energy. Then the absorption intensity of the special pair monomers is mainly in the low energy band P(−) of the two excitonically split special pair states. However, the state P(+) has the possibility to borrow intensity from other pigments that are nearby and have a similar energy. According to our model studies, this is only possible if the exciton energy of the state P(+) is below the energy of the accessory monomers—i.e., for $0 < V_p < -E_p$. At the same time, the agreement with the experimental CD spectrum is lost (12).

In our calculation, the exciton state P(+) carries only little intensity in absorption and is strongly mixed with the exciton states of BP_L and BC_{MA}. It appears at an energy of 811 nm (Table 2) between the states of the BP and BC_A molecules. On the other hand, the lowest exciton state of the accessory monomers from BC_{LA} appearing at 838 nm has a considerable admixture (35%) from the special pair molecules (Table 2). Hence, the shoulder observed at 850 nm in absorption spectra at low temperature (20) is most likely due to this state. At low temperature, the energy of this state is diminished.

The Circular Dichroism Spectrum

The CD spectrum in Fig. 4 exhibits a broad positive lobe at 960 nm, which is due to the exciton state P(−). At high energies, a much sharper negative and positive lobe from the two accessory monomers follow. Apparently, the two BP molecules do not contribute significantly to the experimental CD spectrum (8). This is in contrast with the calculated CD spectrum, where the BP_M molecule gives rise to the negative lobe at 790 nm. In addition, the experimental CD spectrum of the Q_y bands contains more positive than negative ellipticity and is, therefore, not conservative, in contrast to our simple theoretical description (Eqs. 5–7). This may also relate to the discrepancy of the CD spectra at 790 nm. This problem could not be resolved by using an exciton model that also includes the Soret bands. Their influence is <8% (12). The rotational strength of the exciton state P(−) at 960 nm is 3.7 Debye Bohr magneton, which is 15% above the value given in ref. 9.

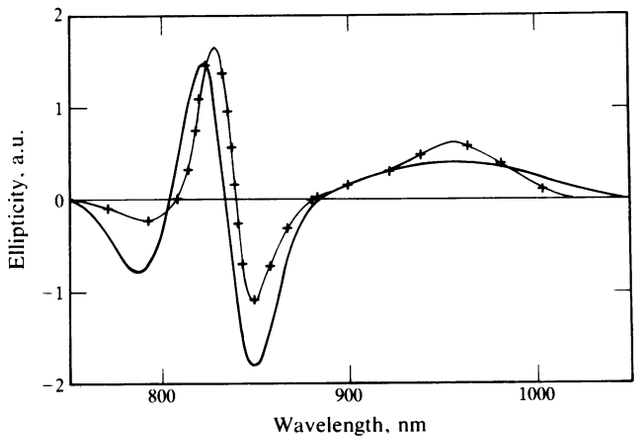

FIG. 4. Circular dichroism spectrum of RCs in solution. +—+, Experiments taken from ref. 8; —, theoretical data.

The Absorbance Changes

We now turn to the observed changes of absorption induced by illumination with light at λ = 970 nm (Figs. 2 and 3). These spectra are mainly determined by bleaching of the lower exciton state P(−) of the special pair and Stark shift of the accessory monomers to higher energies (200 cm^{-1}) because of the presence of a positive charge at the special pair monomers after illumination. Bleaching of the exciton state P(−) gives rise to the negative lobe at 960 nm. In Fig. 2*b*, this negative lobe does not appear, because for all RCs in the unit cell, the special pair state at 960 nm has nearly a vanishing transition dipole moment along the polarization of the probing light ($E_{pr} \parallel z$). In Fig. 3*b*, the negative lobe at 960 nm is lacking, since the orientation of the RCs in the unit cell is such that the special pair state of one-half of the RCs is bleached by the actinic light while the probing light interrogates the other half. The Stark shift of the accessory monomers to higher energies is responsible for the negative lobe at 850 nm and for the positive lobe at 810 nm. The BPs do not play a role.

The experimental absorption spectra and light-induced absorbance changes exhibit line shapes of the special pair state at 960 nm, which differ in the high energy wing. This difference can be related to unhomogeneous broadening of the 960-nm line. In the present experiments, essentially the long wave length part of this state is bleached. Then the negative lobe of the absorbance change at 960 nm (Fig. 3 and 4) displays the line shape of this part only. The details of the line shape of this state seem to depend on preparation and age of the RCs. The broad wing at 930 nm increases with aging of the sample. This points to the possibility that this wing corresponds to the special pair state P(−) of reaction centers in a slightly different protein environment.

The Q_x Bands

The Q_x bands do not depend significantly on the structure of the RC, since the dipolar interactions are 10 times smaller than for the Q_y bands (4). The corresponding transition dipole moment determines the intensity of the Q_x bands relative to the Q_y bands. Fig. 2 reveals that the calculated intensity at 540 nm, where the BP monomers absorb (16) is too low. This is the frequency regime, where the hemes of *c*-type cytochrome of the RC absorb very strongly. The calculated absorbance changes in the Q_x bands are due to the special pair states only. They agree well with the experimental data if the diagonal energies of the BC monomers of the special pair E_p are 200 cm^{-1} below the energies of the accessory monomers. Accordingly, the Q_x bands of the special pair are around 610 nm and the Q_x bands of the accessory monomers are around 605 nm. The different polarization dependence of the bleaching of the special pair state around 610 nm is due to the different orientations of the corresponding dipole moments of the pigments and to the fact that only the Q_y band was excited by the actinic light.

Conclusions

The present study provides a consistent picture of structural and spectroscopic information. The theoretical analysis allows an unambiguous assignment of the exciton states in the spectrum to the different pigments of the reaction center. As a result, we can clarify several points. (*i*) The upper exciton state of the special pair P(+) carries practically no intensity in an absorption spectrum. (*ii*) The upper exciton state of the special pair P(+) is vital for an understanding of the circular dichroism spectrum, and it is situated between the bacteriopheophytins and and the accessory monomers of the reaction center. (*iii*) The pair of bacteriopheophytins and accessory bacteriochlorophylls from the two branches are spectroscopically rather unequivalent.

We thank Prof. R. Huber, Prof. M. E. Michel-Beyerle, and Prof. H. Scheer for valuable discussions. We are grateful to Dr. A. Scherz who made his experimental data available to us prior to publication. This work was supported by the Deutsche Forschungsgemeinschaft under the project "Primary Processes in Bacterial Photosynthesis" (SFB 143).

1. Feher, G. & Okamura, M. Y. (1978) in *The Photosynthetic Bacteria*, eds. Clayton, R. K. & Sistrom, W. R. (Plenum, New York), pp. 349–386.
2. Hoff, A. J. (1982) in *Molecular Biology, Biochemistry and Biophysics*, ed. Fong, F. K. (Springer, Berlin), Vol. 35, pp. 80–151, 347–425.
3. Parson, W. W. (1982) *Annu. Rev. Bioeng.* **11**, 57–80.
4. Pearlstein, R. M. (1982) in *Photosynthesis: Energy Conversion by Plants and Bacteria*, ed. Govindjee (Academic, New York), Vol. 1, pp. 293–330.
5. Michel, H. (1982) *J. Mol. Biol.* **158**, 567–572.
6. Zinth, W., Kaiser, W. & Michel, H. (1983) *Biochim. Biophys. Acta* **723**, 128–131.
7. Deisenhofer, J., Epp, O., Miki, K., Huber, R. & Michel, H. (1984) *J. Mol. Biol.* **180**, 385–398.
8. Philipson, K. D. & Sauer, K. (1973) *Biochemistry* **12**, 535–539.
9. Shuvalow, V. A. & Asadov, A. A. (1979) *Biochim. Biophys. Acta* **545**, 296–308.
10. Zinth, W., Knapp, E. W., Fischer, S. F., Kaiser, W., Deisenhofer, J. & Michel, H. (1985) *Chem. Phys. Lett.* **119**, 1–4.
11. Zinth, W., Sander, M., Dobler, J., Kaiser, W. & Michel, H. (1985) in *Antennas and Reaction Centers of Photosynthetic Bacteria-Structure: Interactions and Dynamics*, ed. Michel-Beyerle, M. E. (Springer, Berlin), in press.
12. Knapp, E. W., Fischer, S. F. (1985) in *Antennas and Reaction Centers of Photosynthetic Bacteria-Structure: Interactions and Dynamics*, ed. Michel-Beyerle, M. E. (Springer, Berlin), in press.
13. Hemenger, R. P. (1978) *J. Chem. Phys.* **68**, 1722–1728.
14. Warshel, A. (1979) *J. Am. Chem. Soc.* **101**, 744–746.
15. Scherz, A. & Parson, W. W. (1984) *Biochim. Biophys. Acta* **766**, 653–665.
16. Davis, M. S., Forman, A., Hanson, L. K., Thornber, J. P. & Fajer, J. (1979) *J. Phys. Chem.* **83**, 3325–3332.
17. Davydov, A. S. (1971) *Theory of Molecular Excitons in Molecular Crystals* (Benjamin, New York).
18. Seftor, R. E. B. & Thornber, J. P. (1984) *Biochim. Biophys. Acta* **764**, 148–159.
19. Van Der Rest, M. & Gingras, G. (1974) *J. Biol. Chem.* **249**, 6446–6453.
20. Vermeglio, A. & Paillotin, G. (1982) *Biochim. Biophys. Acta* **681**, 32–40.
21. Thornber, J. P., Cogdell, R. J., Seftor, R. E. B. & Webster, G. D. (1980) *Biochim. Biophys. Acta* **593**, 60–75.